



Influence of fibers on desiccation cracks in sodic soil

Shichong Yuan¹ · Binbin Yang² · Jiawei Liu¹ · Bin Cao²

Received: 4 May 2020 / Accepted: 2 February 2021 / Published online: 10 February 2021
© Springer-Verlag GmbH Germany, part of Springer Nature 2021

Abstract

Drying shrinkage of soil contaminated by alkaline solutions in ecologically fragile areas is a key issue that affects the strength, stability, and permeability of contaminated soil. Reinforcement with polypropylene fibers is a common physical treatment method. This paper presents experimental investigations of the shear strength, permeability, formation, and development of desiccation cracks in sodic soil with four different contents of polypropylene fibers: 0%, 2%, 4%, and 8%. The shear strength and permeability coefficient were tested by the SLB-1 triaxial shear permeability tester. Meanwhile, a series of crack images and water content evolution were obtained during free desiccation tests with self-designed monitoring equipment. The dynamic changes in the cracks are then quantitatively analyzed by using digital image processing and geographic information system (GIS) analysis. The experimental results show that shear strength increases and permeability coefficient decreases with the increase of fiber content. The evaporation process with different polypropylene fiber contents has three stages, namely, Stages I, II, and III that are in accordance with the slope of the evaporation curve. However, the polypropylene fiber content has little effect on the total duration of crack development. The crack development process has three stages. The crack ratio, fractal dimension, and average width decrease as the polypropylene fiber content increases. The fractal dimension gradually and linearly increases with time. The fractal dimensions of the cracks are reduced with increased polypropylene fiber content, which indicates that polypropylene fibers can inhibit the development of soil cracking. Because the elastic modulus of the fibers is very high, it is difficult for the fibers to be pulled out from the soil during cracking. Therefore, friction is produced at the interface between the fibers and soil particles, which can inevitably inhibit the relative sliding of the fibers and share the tensile stress caused by the structural shrinkage in the soil. Therefore, polypropylene fibers can dramatically improve the stability and integrity of soil, similar to a “bridge.” In conclusion, these research results provide an important explanation for dealing with alkali-contaminated foundations and soils.

Keywords Desiccation cracks · Fractal dimension · Image processing · Sodic soil · Fiber-reinforced soils

Introduction

Currently, soil contaminated by alkaline solutions is widely distributed in tropical and cold temperate regions, coastal and inland areas, and areas that are high in humidity or have an arid desert climate and cover 954.38 million ha of dry land on Earth. Drying shrinkage of soil contaminated by alkaline solutions in ecologically fragile areas in western China is currently a key issue in engineering and construction projects. Soil contaminated by alkaline solutions is considered to be a typical degraded soil that will affect the engineering and environmental properties of the ground. Due to the evaporation of water from the soil surface in arid climates, the salt will accumulate inside the soil, causing shrinkage, deformation, and cracking (Abdullah et al. 1997; Yang and Yuan 2019a).

The change and remediation of physical and textural properties of contaminated soil are popular topics in research on

✉ Binbin Yang
yangbinbin@xcu.edu.cn

✉ Jiawei Liu
liujiawei@cumt.edu.cn

Shichong Yuan
yuanshichong@cumt.edu.cn

Bin Cao
discipline1997@hotmail.com

¹ School of Resources and Geosciences, China University of Mining and Technology, 1 University Rd, Xuzhou 221008, Jiangsu, China

² School of Civil Engineering, Xuchang University, No.88 Bayi Rd, Xuchang 461000, Henan, China

the cross-industry of engineering geology and materials (Koooper and Mangnus 1986). Combining physical, chemical, biological, and ecological methods for improving the contaminated soil is the trend of future development. The physical and mechanical properties in the crack formation and development process of alkali-contaminated foundations and soils greatly affect the structural strength, moisture, heat, and solute transport model in unsaturated soil (Agarwal 1968; Barbour and Yang 1993; Richards 1969).

The distribution and connectivity of desiccation crack networks are two important factors that control or affect the diffusion and transport paths of water, heat, and pollutants in soil. Along with the development of engineering construction, modern agriculture, and geocological environments, an increasing number of studies have focused on the formation mechanism, development process, and improvements of desiccation soil cracks. In slope engineering, for example, desiccation cracks cause increases in soil permeability and reduce the strength and stability of soils. Moreover, the weathering and erosion of slope soils are increased. As a result, landslides are easily triggered (Baker 1981; Meisina 2006). Clay soils are often used as a buffer material for the lining of landfills in environmental engineering applications. However, the desiccation in clay soils and subsequent surface shrinkage results in the formation of cracks on the soil surface. As cracks develop in clay soils, the risk of pollutant leakage increases, which threatens the environment (Rowe et al. 2004; Yesiller et al. 2000; Cripps and Parmar 2015). Therefore, there is great scientific merit and practical value in examining desiccation cracks in soil to prevent environmental pollution and improve the slope stability.

Theoretical research work on desiccation cracks is rare and is mainly based on elasticity theory and fracture mechanics (Lachenbruch 1962; Morris et al. 1992). Fracture mechanics is widely applied in crack analyses of solid materials and soil (Yang and Yuan 2019b). For instance, Konrad and Ayad (1997) formulated a model to predict the average spacing between cracks in cohesive soils that are in the process of desiccation based on linear elastic fracture mechanics. Towner (1987) experimentally examined desiccation cracking in remolded clay with different initial water contents and found that the particles of clay soils that shrink in unrestricted directions allow internal equilibrium in terms of the x , y , and z dimensions as the water pressure acts in an isotropic manner and therefore reduces the constrained tension. With the development of computer technology, discrete element and finite element methods have been used to simulate crack networks (Péron et al. 2006). Horgan and Young (2000) proposed a model for soil water loss and cracking by establishing a number of geometric parameters related to fracture development. Chen and Bulut (2017) proposed a numerical model to study the effects of desiccation cracks on the moisture diffusion coefficient of unsaturated soils. They offered

guidelines to estimate the field diffusion coefficient with a given crack width and depth.

In recent years, qualitative and quantitative studies on desiccation cracks in soils have mainly focused on the morphological characteristics of the cracks. The geometrical structure and process of surface desiccation cracks resulting from different factors in clayey soils have been studied by Tang et al. (2008, 2011a, 2011b), in which the development of desiccation cracks and the evaporation of water in clayey soils were depicted as four and three stages, respectively, and the Crack Image Analysis System (CIAS) software was developed to analyze desiccation crack patterns. Sanchez et al. (2013) used a 2D profile laser coupled with a motion controller to investigate desiccation cracks in soils. Levatti et al. (2017) used a ground-penetrating radar (GPR) system to detect 3D cracking in drying soils and found that cracks with a width of 1 or 2 mm can be detected. An image processing method was then proposed and used to perform simultaneous and continuous quantifications of the vertical and radial strains and crack area (Auvray et al. 2014).

In this context, many soil improvement methods have been developed in the geotechnical engineering context, including physical, chemical, and biological treatment technologies. Chemical grouting is a widely used technique to reinforce loose soil and sand layers. Zhang (2011) found that during the process of sand compaction, infiltration, and fracturing, variations in the diffusion concentration of chemical grout in sand greatly influences its permeability. Liang et al. (2019) presented an experimental investigation of the patterns of the propagation of chemical grout in an inclined fracture model to control sand and water flow. Microbial induced calcium carbonate precipitation (MICP) technology has been adopted to improve the water stability and erosion resistance of clayey soil (DeJong et al. 2013; Teng et al. 1998; Martinez et al. 2013). Discrete staple fiber reinforcement is a new and highly applicable soil improvement technology developed in recent years. Because fibers have the advantages of high strength, strong acid and alkali resistance, good dispersion, and easy mixing, they can be used to improve polluted soil (Chandrasekaran et al. 1989; Gupta and Kumar 2016; Kumar et al. 2007; Tang et al. 2007). Currently, many research results show that the addition of discrete short fibers can substantially improve the compression strength, shear strength, tensile strength, and bearing capacity of soil, and the effect of the reinforcement is more substantial when the fibers are used together with cement, lime, and other inorganic binders. However, these materials for reinforced cracked soils generally increase the soil permeability. Therefore, geotextiles are widely used for slope stabilization, vegetation management, and soil erosion control (Dayte and Gore 1994; Sutherland 1998; Mitchell et al. 2003). Arora and Kumar (2019) presented an experimental and numerical investigation carried out on a two-layered soil system that contained an

unreinforced/randomly distributed fiber-reinforced pond ash (RDFP) layer overlying a soft clay layer, and the results showed that there was a substantial amount of improvement in the ultimate bearing capacity. Nguyen and Fatahi (2016) formulated a constitutive model (C3F Model) to simulate the behavior of fiber-reinforced cement-treated soil and captured broken cementation bonds and ruptured fibers based on a nonlinear failure envelope and critical state line (CSL).

The main objective of this research was to investigate how the polypropylene fiber content inhibits the development of desiccation cracks in sodic soils in the Xinjiang Uygur Autonomous Region in China. The characteristics of desiccation cracks in sodic soils with different polypropylene fiber contents were investigated through laboratory experiments. A series of crack images and water content evolution were obtained during free desiccation tests by self-designed monitoring equipment. The strength and permeability of the samples with different polypropylene fiber contents were tested using an SLB-1 triaxial shear permeability tester. The dynamic changes in the cracks were then quantitatively analyzed by using digital image processing and geographic information system (GIS) analysis. In conclusion, these research results provided an explanation for dealing with alkali-contaminated foundations and soils.

Materials and methods

Materials

Once NaOH, Na₂CO₃, or other alkaline solutions penetrate into the foundation soil, they will cause uneven settlement of the foundation and cracking, tilting, sinking, uplifting, or even collapsing of the structures on it. Furthermore, the chemical reaction between NaOH and CO₂ will generate Na₂CO₃. As the ambient temperature changes and the wet and dry conditions alternate, water-containing calcium carbonate crystals will eventually be formed, causing the foundation soil to swell.

Sodic soil samples were taken from a site in the Xinjiang Uygur Autonomous Region, which is a typical ecologically fragile area in Western China. Xinjiang is located in the core area of the Silk Road Economic Belt. The promotion and influence of “The Belt and Road Initiative” engineering

construction are rapidly developing in this region. The study area belongs to the middle temperate continental arid climate zone, with a mean annual temperature of 7.3 °C and an average annual rainfall of 236 mm. When the soil is polluted by alkaline solutions, it will corrode the concrete surface and affect the stability of the foundation. The depth from which the soil samples are taken is approximately 0.3 to 0.5 m. The basic physical and textural properties of the soil samples in the laboratory are listed in Table 1, according to the standard for Engineering Classification of Soil (GB/T 50145-2007, in China). The soil samples are classified as low liquid limit silty clay. Sodium carbonate powder was selected as the pollutant in the experiment and added to the soil slurry with a content of 0.5% of the mass of the soil sample.

Four different contents of polypropylene fibers, 0%, 2%, 4%, and 8%, were mixed in the saturated slurries to reinforce the sodic soil. The length of the polypropylene fiber was approximately 6 mm. Polypropylene fibers are a kind of high molecular weight compound that are made of propylene and polymerized by a special process (CH₃—CH=2CH₂). They have high strength, heat resistance, acid and alkali resistance, and non-water absorption. The basic properties and characteristics of the polypropylene fiber used in this experiment are shown in Table 2. Three-phase diagrams of the normal soil, sodic soil, and fiber-reinforced sodic soil are shown in Fig. 1a, b, and c, respectively.

Methods

Experimental program

In this experiment, eight-round glass containers were used to hold the saturated slurry with different fiber contents of polypropylene fibers, and one contrast sample was produced for each content. The diameter of each round glass container was 20 cm, and the height was 5 cm. The sodic clay taken from the site was air-dried, crushed, and sieved passing through a 2 mm sieve in the laboratory. The natural moisture content of the soil samples measured by the oven-drying method was 8.5%. To ensure that each slurry was adequately uniform, the gravimetric water content for sample preparation in the saturated slurry was 105%. Sodium carbonate (0.5%) and four different contents of polypropylene fibers (0, 2, 4, and 8%) were added to the saturated slurries and stirred well in the same direction.

Table 1 Basic physical and textural properties of the soil samples

Specific gravity	Maximum dry density (g/cm ³)	Optimum moisture content (%)	Liquid limit	Plastic limit	Shrinkage limit	Plasticity index	pH	Granulometric composition (%)		
								Clay	Silt	Sand
2.75	1.66	23.5	35.5	18.8	11.5	16.7	10.5	55	35	10

Table 2 Physical properties and characteristics of the polypropylene fiber

Classification	Length (mm)	Diameter (um)	Density (g/cm ³)	Filament number (dtex)	Tensile strength (MPa)	Ultimate elongation (%)	Elasticity modulus (GPa)	Melting point (K)
Bundle monofilament	6	18-48	0.91	≤2.2	>486	>15	>4.8	442.15

Free desiccation tests were performed to examine the effect of polypropylene fibers on the evaporation and crack development of sodic soil. A schematic diagram of the monitoring equipment is shown in Fig. 2a. A digital camera and electronic balance were used to record the development of surface cracks and the rate of water loss in the soil samples at the same time intervals. The measurement accuracy of the electronic balance was 0.001 g. After the free desiccation tests, the crack images, weight change, and drying time data of each soil sample were recorded and stored in a laptop computer.

The strength and permeability of the samples with 0, 2, 4, and 8% polypropylene fibers were tested using an SLB-1 triaxial shear permeability tester, as shown in Fig. 2b. The main parameters of the SLB-1 triaxial shear permeability tester were as follows: axial load 0–20 kN (±1%), loading rate 0.002–4 mm/min (±10%), confining pressure 0–1.99 MPa (±0.05%), back pressure 0–0.99 MPa (±0.05%), constant permeation flow 1–30 ml/min, and volume change 0–50 ml. In this experiment, the confining pressure was 0.1 MPa, the permeation flow was 5 ml/min, and the loading rate was 2 mm/min. After the soil sample and fiber were fully mixed, the soil was compacted in three layers with 94 blows in each layer and sealed with a plastic film for 7 days (GB/T50123, in China).

Image processing and parameter calculation

To extract the crack networks on the sample surface, these original crack images obtained by the digital camera need to be converted to binary images. A geographic information

system (GIS) was used to process these original images, and details of this process can be found in the work by Abd El-Halim (2017), Ren et al. (2015), and Yang et al. (2019a). The extracted crack images were processed by edge detection and threshold segmentation to obtain the binary images. These binary images were imported into the ArcGIS software and transformed into GIS layers that represent the surface features by using points, lines, and polygons. The parameters of the desiccation cracks, including the crack length, width, area, and direction, were counted and calculated by using ArcGIS tools.

The development of cracks is accompanied by a constant change in the water content, and the water content can be calculated as:

$$w = \frac{m - m_s}{m_s} \times 100\%, \quad (1)$$

where w is the water content, m is the saturated slurry mass, and m_s is the soil dry mass.

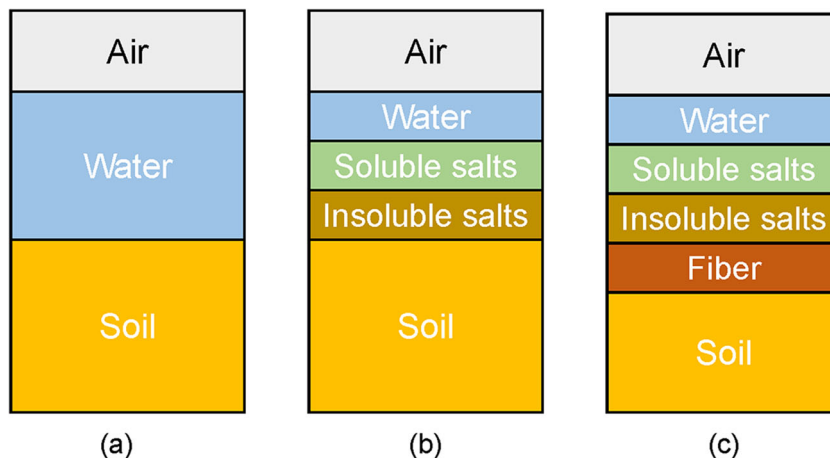
The crack ratio is an important parameter for quantitatively examining the development of desiccation cracks and can be calculated as:

$$\mu = \frac{S_0}{S} \times 100\%, \quad (2)$$

where μ is the crack ratio, S is the cross-sectional area of the round glass container, and S_0 is the total crack area.

The concept of fractals was initiated by the French mathematician Manderbrot in 1975. It has been studied

Fig. 1 Three-phase diagram of normal soil (a), sodic soil (b), and fiber-reinforced sodic soil (c)



and employed for many applications, such as irregular curves with similarity, irregular figures with inversion, and self-reflecting fractal sets. The fractal dimension is used to characterize self-similarity, which is when there are similarities in form, function, and information between the part and the whole. In the study of the crack structure, three definition methods are mainly used: the capacity dimension (D_k), information dimension (D_i), and similarity dimension (D_s). They are defined as follows:

$$D_k(C) = \lim_{\varepsilon \rightarrow 0} \frac{\ln N(\varepsilon)}{\ln(1/\varepsilon)} = - \lim_{\varepsilon \rightarrow 0} \frac{\ln N(\varepsilon)}{\ln \varepsilon} \tag{3}$$

where $N(\varepsilon)$ is the number of units that are covered by the box with a length of ε , and ε is the length of the box.

$$D_i(C) = \lim_{\varepsilon \rightarrow 0} \frac{I(\varepsilon)}{\ln(1/\varepsilon)} = - \lim_{\varepsilon \rightarrow 0} \frac{I(\varepsilon)}{\ln \varepsilon} \tag{4}$$

$$I(\varepsilon) = \sum_{i=1}^{N(\varepsilon)} P_i \ln(1/P_i) \tag{5}$$

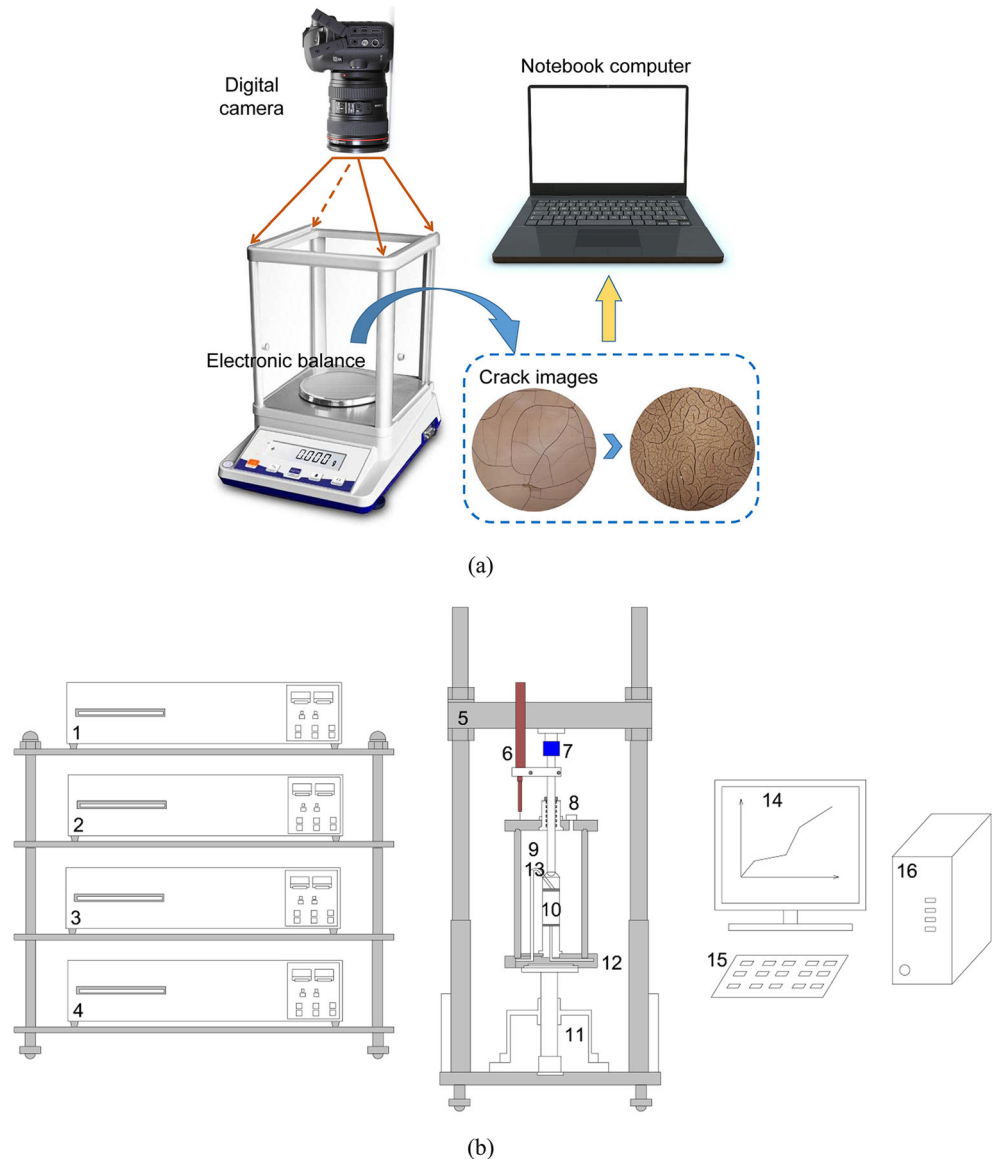
where ε is the length of the box and P_i is the probability that the crack point is on the i^{th} square grid.

$$D_s(C) = - \frac{\log N(\varepsilon)}{\log(\varepsilon)} \tag{6}$$

where $N(\varepsilon)$ is the number of units that are covered by the box with a length of ε .

Grid covering is the most commonly used method (employed also in this paper) for calculating the fractal dimension of D_s (Fig. 3). The grid cell size ε is used to cover the crack networks, and the number of grid cells containing the

Fig. 2 Equipment used in the experiment: **a** schematic diagram of the monitoring equipment; **b** SLB-1 triaxial shear permeability tester 1. Axial pressure controller, 2. Confining pressure controller, 3. Upper back pressure controller, 4. Lower back pressure controller, 5. Support, 6. Displacement sensor, 7. Stress sensors, 8. Air vent, 9. Pressure chamber, 10. Sample, 11. Lifting platform, 12. Water inlet, 13. Water outlet, 14. Display, 15. Keyboard, and 16. Mainframe



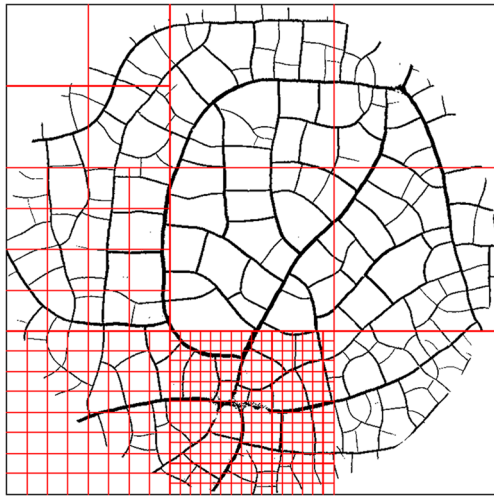


Fig. 3 Schematic diagram of the grid cell division

crack point $N(\varepsilon)$ is recorded. Then, coverage is continued with a grid cell size r_i , which is reduced by a certain proportion to obtain the number of grid cells containing the crack point $N(\varepsilon)$. The linear fitting slope of $\ln N(\varepsilon) - \ln(\varepsilon)$ is the similarity dimension D_s . r_i can be obtained as follows:

$$r_i = \frac{1}{2^n} r_0, (i = n = 1, 2, 3, 4, 5, \dots) \quad (7)$$

Results and analyses

Strength and permeability

Figure 4 shows the relationship between the strength, permeability coefficient, and fiber content tested by the SLB-1 tri-axial shear permeability tester. The results show that the strength increases with increasing fiber content; however, the permeability coefficient shows the opposite trend and

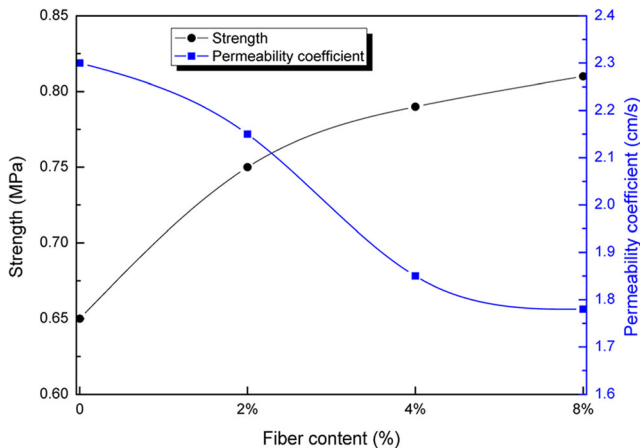


Fig. 4 Strength and permeability coefficient of the soil samples with different fiber contents versus the fiber content

decreases with increasing fiber content. Due to the large specific surface area of the polypropylene fibers, the randomly distributed fibers in the soil sample form a spatial network of random support systems inside the soil sample, which acts as an “anchor rod.” However, the interface between the polypropylene fibers and soil particles is the dominant channel for water level migration.

Evaporation process

Evaporation from bare soils is a main component of the hydrologic cycle in nature. It is not only responsible for desiccation cracks on the soil surface but may also cause large-scale soil salinization, particularly in arid and semiarid regions. Figure 5 shows the change process of the water content during drying with different polypropylene fiber contents. It can be observed that the water content is reduced during drying for all samples. Because the water content for sample preparation in the saturated slurry is 105%, the soil sample is in an oversaturated state. When the evaporation capacity exceeds

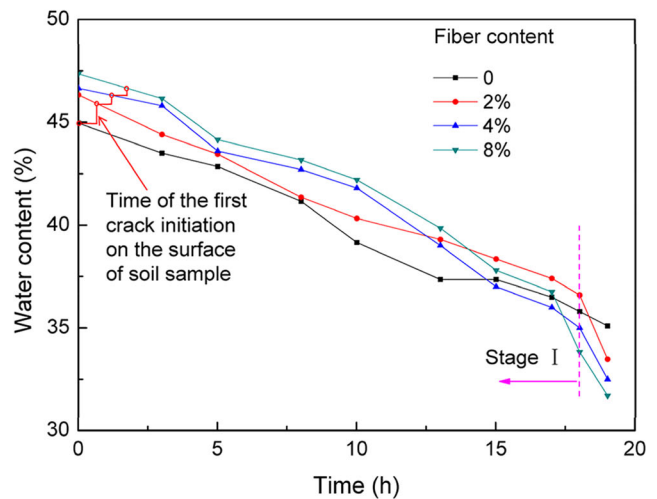
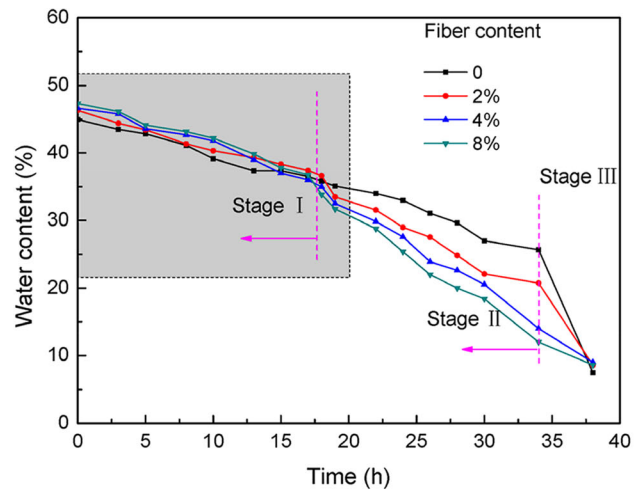


Fig. 5 Water content change process during drying for different fiber contents

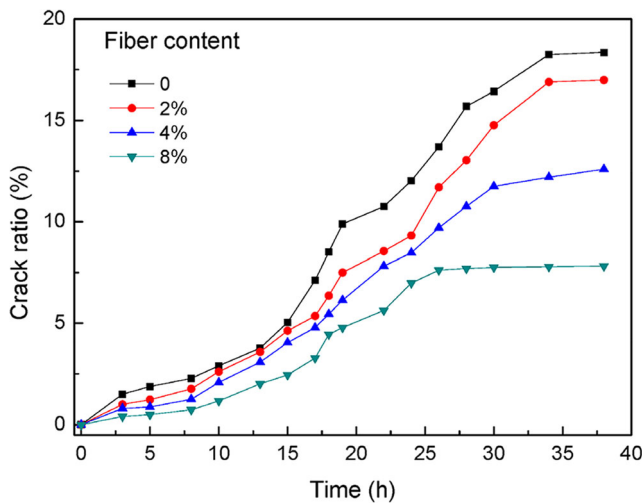


Fig. 6 Crack ratio versus time for different polypropylene fiber contents

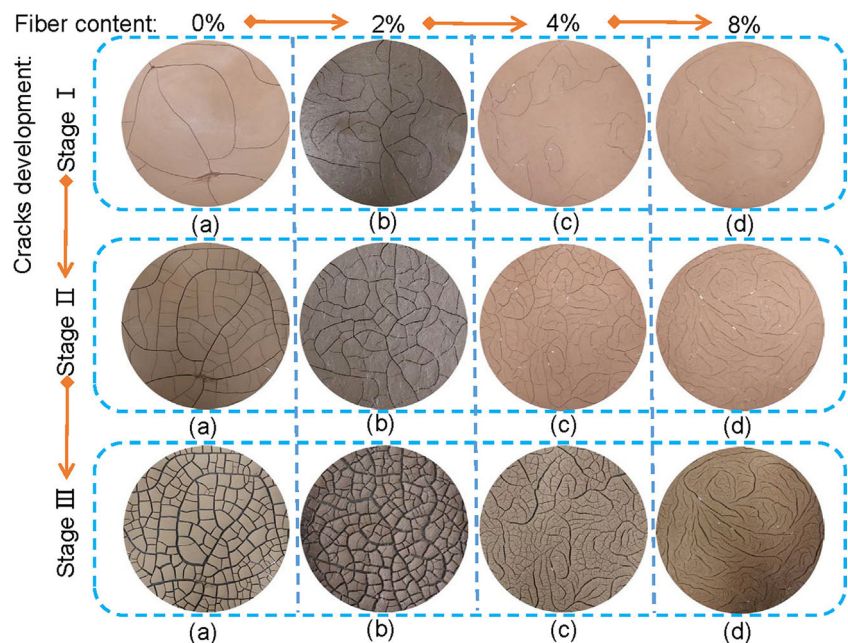
a certain value, cracks on the soil surface begin to appear. The water content of crack occurrence slightly differed between the soil samples; moreover, the water content decreases slightly with increasing fiber content. However, the fiber content has little effect on the total duration of crack development.

The variation process in water content versus time can be examined in three stages that are in accordance with the slope of the curve, as shown in Fig. 5. In the early stage of the free desiccation tests, the relative evaporation rates of different fiber contents are approximately equal, and this stage lasts approximately 18 h. When the free desiccation test duration is 18–34 h, the evaporation process reaches the second stage. At this stage, the

relative evaporation rate accelerates with increasing fiber content. At the third stage, the water contents of all the soil samples decrease quickly. The duration of the third stage is only approximately 4 hours. When the water contents of all the soil samples is reduced to approximately 7.5%, the water content change will not cause further cracking in the surface of the soil sample.

During the first stage of the evaporation process, the samples were in a saturated state, and the pores were filled with free water. Therefore, the main loss of water was the free water on the surface of the samples. Hence, the different contents of polypropylene fibers had little effect on the evaporation rate at the first stage. With continuous evaporation, the water would decrease from shallow to deep soil samples through capillary action. This process could be simplified to two-dimensional nonsteady upward flow. The water content was gradually reduced, and therefore, the crack ratio correspondingly increased at different times. The variations in the crack ratio versus time for different fiber contents are shown in Fig. 6. Although the polypropylene fibers themselves do not absorb water, the interface between the fibers and soil particles becomes the dominant path of water migration from the lower parts of the soil samples. Therefore, polypropylene fibers can increase the effective porosity of the soil, which can promote the evaporation of water. As the crack rate and crack depth gradually increase, the contact area between the soil and air increases; therefore, the residual free water will be quickly reduced in the third stage. However, some of the strongly bound water remains in the micropores of the soil.

Fig. 7 Three stages of development for desiccation cracks. Soil samples: **a** no polypropylene fiber, **b** 2% polypropylene fiber, **c** 4% polypropylene fiber, and **d** 8% polypropylene fiber



Crack development process

Figure 7 shows pictures of the typical experiments, in which a series of images of desiccation crack dynamic development are consecutively presented. Three stages of crack development can be observed from the experimental results: Stages I, II, and III. In Stage I, the first isolated fissure is called the main crack. When the adjacent main cracks intersect each other, the soil surface is divided into several large polygonal blocks. In Stage II, bifurcation of the main cracks begins to take place so that the bifurcation cracks connect to the existing cracks to form a polygonal network. At Stage III, all the polygonal blocks remain stable and unchanged, and the cracks gradually widen until they stabilize.

The fractal dimension is a quantitative parameter that describes the similarities and relevant features among the apparently random but unique crack networks in the soil surface. Figure 8 shows the variations in the fractal dimension versus time with different polypropylene fiber contents. The fractal dimension gradually and linearly increases with time, and the fitting formulas are shown in Table 3. The fractal dimensions of the cracks are reduced with increasing polypropylene fiber content, which indicates that polypropylene fibers can inhibit the development of soil cracking.

During the drying process of sodic soil, the decrease in the water content will lead to the generation of suction, forming a tensile stress field inside the soil. When the tensile stress exceeds the tensile strength of the soil, cracks will be produced. The tensile strength of polypropylene fiber-reinforced soil increased during the shrinkage of the sodic soil. Because the elastic modulus of the polypropylene fibers and soil are different, mutual dislocation between the polypropylene fibers and soil may occur during the drying process. Therefore, friction is produced at the interface between the fibers and soil

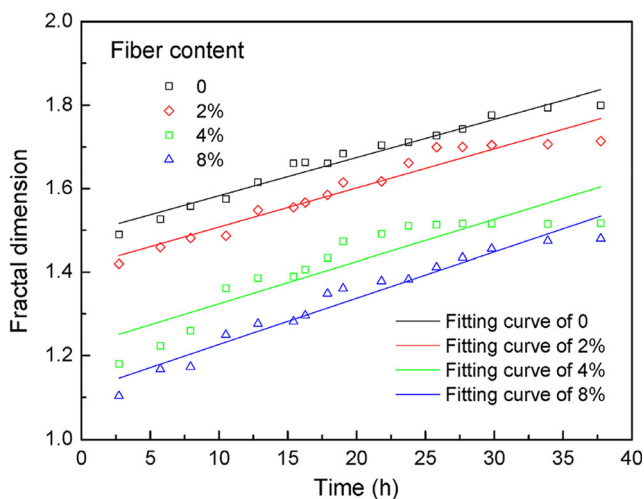


Fig. 8 Fractal dimension versus time for different polypropylene fiber contents

Table 3 The fitting formulas of the fractal dimension and time with different polypropylene fiber contents

Fiber content (%)	Fitting formula	R ²
0	$y=1.4912+0.0091x$	0.96269
2	$y=1.4137+0.0093x$	0.9354
4	$y=1.2232+0.01x$	0.81406
8	$y=1.1158+0.011x$	0.9466

particles, which will inevitably inhibit the relative sliding of the fibers and share the tensile stress caused by the structural shrinkage in the soil. With increasing fiber content, the contact area and friction between the fibers and soil particles also increase accordingly, which makes the reinforcement effect of the fibers in the soil more effective, and the soil can resist a greater tensile stress. In addition, a large number of randomly distributed fibers form a spatial network structure in the soil, which can limit the movement of soil particles and improve the overall structural strength of the soil.

Discussion

The formation and development of desiccation cracks in sodic soil is a complex process that can affect the basic physical and textural properties of soil, such as the compressive strength, permeability, and porosity. Sodic soil is considered to be a typical degraded soil that is widely distributed worldwide and covers 954.38 million ha of dry land on Earth (Yang and Yuan 2019a). Polypropylene fibers have been developed as a reinforcement material to improve the mechanical properties of foundation soil. The tensile strength of the fiber-reinforced soil is expected to be significantly improved and

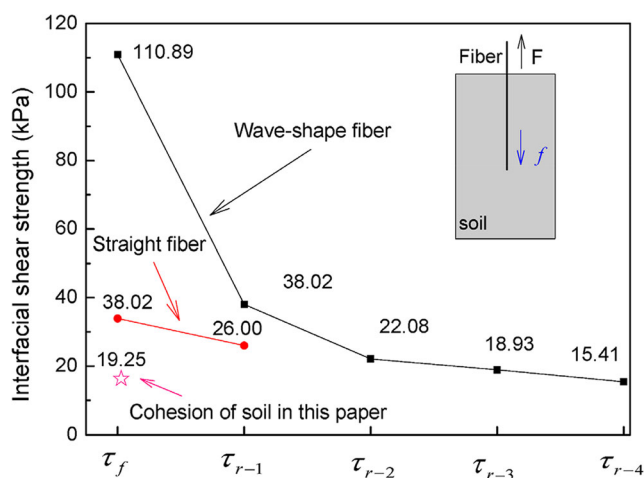


Fig. 9 Interfacial shear strength and residual shear strength of fiber-reinforced soils (Li et al. 2014)

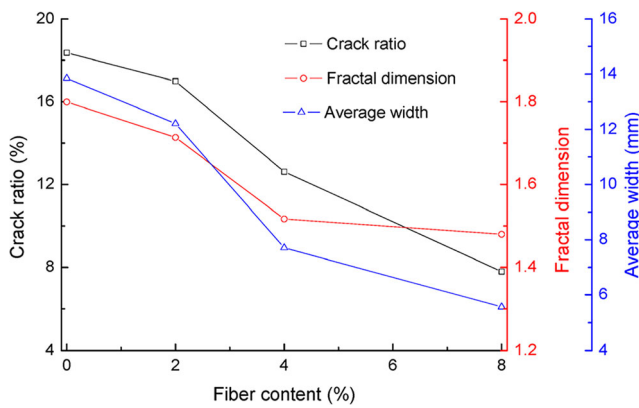


Fig. 10 Crack ratio, fractal dimension, and average width versus the polypropylene fiber content of the final crack image

sufficiently durable. However, the interfacial mechanical interaction between the fibers and soil is the key factor controlling the engineering properties of fiber-reinforced soils. Li et al. (2014) designed an innovative single-fiber pullout test device to quantitatively obtain the interfacial shear strength and residual shear strength of fiber-reinforced soils that are defined as:

$$\tau_f = \frac{F_{max}}{S}, \tag{8}$$

$$\tau_{r-i} = \frac{F_{max-i}}{S}, \tag{9}$$

where τ_f is the interfacial shear strength between the fibers and soil, F_{max} is the maximum tensile force on the fibers during the pull-out test, namely, the first peak value of the fiber pull-out curve, S is the contact area between the fiber and soil; τ_{r-i} is the interfacial residual shear strength, which is the i th peak value of the pull-out curve after the fiber is obviously pulled out, and F_{max-i} is the tensile force on the fiber corresponding to the i th peak of the fiber pull-out curve.

Figure 9 shows the results of the single wave-shape and straight fiber pull-out tests. The interfacial shear strength of the straight fiber-reinforced soils is substantially higher than that of the cohesion of the soil in this study. The crack ratio, fractal dimension, and average width of the final crack image with different polypropylene fiber contents are extracted, and the results are shown in Fig. 10. As the polypropylene fiber content increases, the crack ratio, fractal dimension, and average width continue to decrease, which indicates that the polypropylene fibers can dramatically improve the stability and integrity of the soil, similar to a “bridge.”

Conclusions

To investigate the relationship between different polypropylene fiber contents, 0%, 2%, 4%, and 8%, and the

characteristics of desiccation cracking in sodic soil contaminated with 0.5% sodium carbonate powder, eight soil samples with different polypropylene fiber contents were examined in this study. One contrast sample was produced for each content. The strength increased with increasing fiber content, while the permeability coefficient decreased with increasing fiber content. In-house monitoring equipment was designed, and a series of crack images were obtained at different times. Free desiccation tests were carried out to examine the crack development and water content change in the laboratory setting by applying this monitoring equipment. The ArcGIS software was used to quantitatively describe and analyze the characteristics of the structure of the surface cracks. The main conclusions from this study are summarized as follows.

- (1) The evolution of water content during drying with different polypropylene fiber contents has three stages, namely, Stages I, II, and III, which are in accordance with the slope of the evaporation curve. In Stage I, the relative evaporation rate of different fiber contents is approximately equal, and the loss of water is mainly the free water on the surface of the samples. In Stage II, the relative evaporation rate accelerates with increasing fiber content because the interface between the fibers and soil particles becomes the dominant path of water migration from the lower parts of the soil samples. In Stage III, the free water loss occurs quickly, and the fiber content has little effect on the total duration of crack development.
- (2) The crack development process has three stages. The crack ratio, fractal dimension, and average width decrease as the polypropylene fiber content increases. The fractal dimension gradually and linearly increases with the duration of cracking. The interfacial shear strength of the fiber-reinforced soils is substantially higher than that of the cohesion of the soil in this study. Polypropylene fibers can dramatically improve the stability and integrity of soil, similar to a “bridge.”

Acknowledgements The authors would like to acknowledge the financial support from Henan Key Scientific Research Projects of Colleges and Universities (21A410003) and Xuchang University Scientific Research Fund (2020ZD013). Appreciation is extended to Dr. Xiaoming Zhao for his help during the preparation of this manuscript. We would also like to acknowledge the reviewers for their invaluable comments.

References

Abdullah WS, Al-Zoubi MS, Alshibli KA (1997) On the physicochemical aspects of compacted clay compressibility. *Can Geotech J* 34: 551–559

Agarwal RR (1968) Saline alkali soils in India. Indian Council of Agricultural Research, New Delhi

- Arora S, Kumar A (2019) Bearing capacity of square footing resting on fibre-reinforced pond ash overlying soft clay. *Int J Geosynth Ground Eng* 5(1):3. <https://doi.org/10.1007/s40891-019-0155-0>
- Auvray R, Rosin-Paumier S, Abdallah A, Masroufi F (2014) Quantification of soft soil cracking during suction cycles by image processing. *Eur J Environ Civ Eng* 18(1):11–32. <https://doi.org/10.1080/19648189.2013.840250>
- Abd El-Halim AA (2017) Image processing technique to assess the use of sugarcane pith to mitigate clayey soil cracks: Laboratory experiment. *Soil Tillage Res* 169:138–145. <https://doi.org/10.1016/j.still.2017.02.007>
- Barbour SL, Yang N (1993) A review of the influence of clay-brine interactions on the geotechnical properties of Ca-montmorillonitic clayey soils from western Canada. *Can Geotech J* 30:920–934
- Baker R (1981) Tensile strength, tension cracks, and stability of slopes. *Soils Found* 21(2):1–17
- Chen L, Bulut R (2017) Numerical analysis of the effects of cracks on the moisture-diffusion coefficient of unsaturated soils. *Int J Geomech* 17(8):04017017
- Cripps JC, Parmar KK (2015) Investigations into the self-Healing of desiccation cracks in compacted clays. *Eng Geol Soc Territory* 5: 1327–1331
- Chandrasekaran B, Broms BB, Wong KS (1989) Strength of fabric reinforced sand under axisymmetric loading. *Geotext Geomembr* 8(4): 293–310
- DeJong JT, Soga K, Kavazanjian E, Burns S, Van Paassen LA, Al Qabany A et al (2013) Biogeochemical processes and geotechnical applications: progress, opportunities and challenges. *Geotechnique* 63(4):287–301
- Dayte KR, Gore VN (1994) Application of natural geotextiles and related products. *Geotext Geomembr* 13:371–388
- Gupta D, Kumar A (2016) Strength characterization of cement stabilized and fibre-reinforced clay-pond ash mixes. *Int J Geosynth Ground Eng* 2:32. <https://doi.org/10.1007/s40891-016-0069-z>
- Horgan GW, Young IM (2000) An empirical stochastic model for the geometry of two-dimensional crack growth in soil (with Discussion). *Geoderma* 96(4):263–276
- Kooper WF, Mangnus GA (1986) Contaminated soil. Martinus Nijhoff Publishers, Boston, pp 25–27
- Konrad JM, Ayad R (1997) A idealized framework for the analysis of cohesive soils undergoing desiccation. *Can Geotech J* 34(4):477–488
- Kumar A, Walia BS, Asheet B (2007) Influence of fly ash, lime and polyester fibres on compaction and strength properties of expansive soil. *J Mater Civ Eng ASCE USA* 19(3):242–248
- Lachenbruch AH (1962) Mechanics of thermal contraction cracks and ice-wedge polygons in permafrost. *Geol Soc Am Spec Pap* 70:1–66
- Levatti HU, Prat PC, Ledesma A, Cuadrado A, Cordero JA (2017) Experimental analysis of 3D cracking in drying soils using ground-penetrating radar. *Geotech Test J* 40(2):1–23
- Liang YK, Sui WH, Qi JF (2019) Experimental investigation on chemical grouting of inclined fracture to control sand and water flow. *Tunn Undergr Special Tech* 83:82–90
- Li J, Tang C, Wang D, Shi B, Pei X (2014) Single fiber pullout tests on interfacial shear strength of wave-shape fiber-reinforced soils. *Chin J Geotech Eng* 36(9):1696–1704. <https://doi.org/10.11779/CJGE201409017> (In Chinese, abstract in English)
- Meisina C (2006) Characterisation of weathered clayey soils responsible for shallow landslides. *Nat Hazard Earth Syst* 6(5):825–838
- Morris PH, Graham J, Williams DJ (1992) Cracking in drying soils. *Can Geotech J* 29(2):263–277
- Martinez BC, DeJong JT, Ginn TR, Montoya BM, Barkouki TH, Hunt C, Tanyu B, Major D (2013) Experimental optimization of microbial-induced carbonate precipitation for soil improvement. *J Geotech Geoenviron* 139(4):587–598
- Mitchell DJ, Barton AP, Fullen MA, Hocking TJ, Zhi WB, Yi Z (2003) Field studies of the effects of jute geotextiles on runoff and erosion in Shropshire, UK. *Soil Use Manag* 19:182–184
- Nguyen L, Fatahi B (2016) Behaviour of clay treated with cement & fibre while capturing cementation degradation and fibre failure—C3F Model. *Int J Plast* 81:168–195
- Péron H, Laloui L, Hueckel T, Hu L (2006) Experimental study of desiccation of soil. UNSAT 2006. ASCE Geotech Special Publ 147: 1073–1084
- Richards LA (1969) Diagnosis and improvement of saline and alkali soils. United States Department of Agriculture, Washington
- Rowe RK, Quigley RM, Brachman RW, Booker JR (2004) Barrier systems for waste disposal facilities (No. Ed. 2). Spon Press.
- Ren J, Li X, Zhao K (2015) Quantitative analysis of relationships between crack characteristics and properties of soda-saline soils in Songnen Plain, China. *Chin Geogr Sci* 25:591–601. <https://doi.org/10.1007/s11769-015-0779-5>
- Sanchez M, Atique A, Kim S, Romero E, Zielinski M (2013) Exploring desiccation cracks in soils using a 2D profile laser device. *Acta Geotech* 8(6):583–596
- Sutherland RA (1998) Rolled erosion control systems for hillslope surface protection: a critical review, synthesis and analysis of available data. I. Background and formative years. *Land Degrad Dev* 9:465–486
- Towner GD (1987) The mechanics of cracking of drying clay. *J Agric Eng Res* 36(2):115–124
- Tang C, Shi B, Liu C, Zhao L, Wang B (2008) Influencing factors of geometrical structure of surface shrinkage cracks in clayey soils. *Eng Geol* 101(3):204–217
- Tang CS, Cui YJ, Shi B, Tang AM, Liu C (2011a) Desiccation and cracking behaviour of clay layer from slurry state under wetting-drying cycles. *Geoderma* 166(1):111–118
- Tang CS, Shi B, Liu C, Suo WB, Gao L (2011b) Experimental characterization of shrinkage and desiccation cracking in thin clay layer. *Appl Clay Sci* 52(1):69–77
- Tang CS, Shi B, Gao W, Chen FJ, Cai Y (2007) Strength and mechanical behavior of short polypropylene fiber reinforced and cement stabilized clayey soil. *Geotext Geomembr* 25(3):194–202
- Teng HH, Dove PM, Orme CA, De Yoreo JJ (1998) Thermodynamics of calcite growth: baseline for understanding biomineral formation. *Science* 282(5389):724–727
- Yesiller N, Miller CJ, Inci G, Yaldo K (2000) Desiccation and cracking behavior of three compacted landfill liner soils. *Eng Geol* 57(1): 105–121
- Yang BB, Yuan JH (2019a) Application of fractal theory to characterize desiccation cracks in contaminated clayey soils. *Arab J Geosci* 12(3):85. <https://doi.org/10.1007/s12517-019-4274-7>
- Yang BB, Yuan JH (2019b) Influence of soda content on desiccation cracks in clayey soils. *Soil Sci Soc Am J* 83(4):1054–1061. <https://doi.org/10.2136/sssaj2018.05.0204>
- Zhang GL (2011) High-pressure permeability and microscopic mechanism of chemical grouting solid sand body. China Univ of Mining and Technology, Xuzhou, pp 46–85 (In Chinese, abstract in English)